Structural Optimization of the Special Cold Spraying Nozzle via Response Surface Method

Wenjie Hu[1,2(✉)], Kun Tan[1], Sergii Markovych[1], and Tingting Cao[2,3]

[1] National Aerospace University "Kharkiv Aviation Institute", Kharkiv, Ukraine
[2] School of Aeronautics and Astronautics, Nanchang Institute of Technology, Nanchang, China
[3] Nanchang Hangkong University, Nanchang, China

Abstract. This paper studies a new 90° cold spraying nozzle by response surface method (RSM), which can spray in a limited space. A multi-factor and multi-level response surface regression model with divergent section length, spraying distance, and fillet radius (throat size) as independent variables and powder collision speed as dependent variables are established. The divergent section of the optimized new nozzle is only 12 mm. The results show that the length of the divergent section and spraying distance has a significant effect on the powder impact velocity, but the interaction between the three factors is not obvious. Compared with the numerical simulation data, the error of the optimized parameters is 0.3%; In the range of 400 k–1200 k of propulsion gas, the new 90° nozzle can meet a variety of powder sprayings, such as aluminum (Al), titanium (Ti), nickel (Ni), copper (Cu), magnesium (Mg), and zinc (Zn), which has a good application prospect.

Keywords: Cold spraying nozzle · Multi-factor · Multi-level · Regression model · RSM

1 Introduction

Cold spraying technology (CS) can obtain coatings in the solid-state, which deposited a process of high-speed collision with substrate and formation of coating [1, 2], and it is mainly deposited for restorative [3] and protective coating [4, 5], or additive manufacturing applications [6–9], etc.

In the current study, most researchers focus on straight line nozzles [10–13], resulting in the limited or inconvenient spraying operation in limited Spaces. Hence, to facilitate spraying in a limited space, or areas where linear nozzles cannot be sprayed, this study used the RSM to optimize the design of the 90° nozzle with a rectangular cross-section, the outlet section is rectangular and can be applied to thinner rotating components. After that, three key structural parameters (divergent section length, spraying distance and fillet radius) that affect the powder collision speed are used as independent variables, and the powder collision speed is the dependent variable, a response surface quadratic regression equation is established to analyze the interaction between various factors, and the optimal structure parameters are obtained.

M. Nechyporuk et al. (Eds.): ICTM 2021, LNNS 367, pp. 110–122, 2022.
https://doi.org/10.1007/978-3-030-94259-5_11

2 Theoretical Details of the Nozzle

As shown in Fig. 1a, although the flow field distribution of the circular cross-section is uniform and the turbulence can be minimized, it is not suitable for spraying fine rotating specimens and workpieces.

Therefore, the rectangular nozzle design is considered in this study [14]. Considering the convenience of installation, the upper and lower structures are adopted, and the initial model is shown in Fig. 2.

It is found [15] that when the throat diameter $D_{throat} \geq 6$ mm of the circular section nozzle, a large fluid outlet velocity can be obtained. The rectangular section width is preliminarily 3 mm, so the throat section length $L \geq 9.42$ mm. This study takes the throat with the same cross-sectional area as the benchmark. To achieve the compression effect, the rectangular nozzle in this paper uses the fillet method to compress the cross-sectional area at the 90° corner, and the larger the fillet, the better the compression effect. Through numerical simulation, it is found that when the inlet width of propulsion gas is 16 mm and the fillet exceeds 30 mm, the throat compression radius is close to 10 mm. The primary fillet radius $R = 18$ mm and the cross-section width of the throat inlet is 16 mm, At this time, the throat has a certain compression effect.

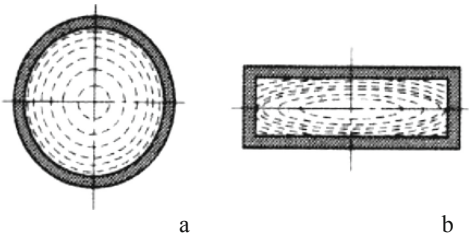

Fig. 1. Three different nozzle cross-sections: a - circular; b - rectangular [14]

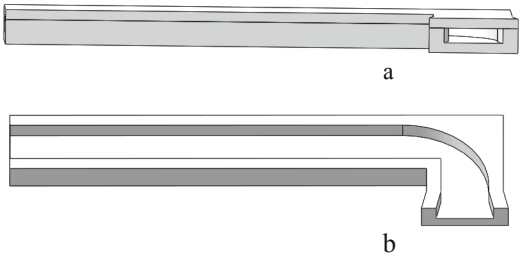

Fig. 2. The actual picture of the initial model of the 3D model: a - the combination of the upper and lower parts; b - only the lower part

3 Theoretical Details of the Single Factor

Since the particle acceleration process is mainly affected by the main drag force of the air flow, this paper assumes that the powder are spherical particles with smooth surface (Fig. 3), and the aerodynamic drag force formula is shown in Eq. 1:

$$F = \frac{1}{2} C_D \rho_g (v_g - v_p)^2 S \tag{1}$$

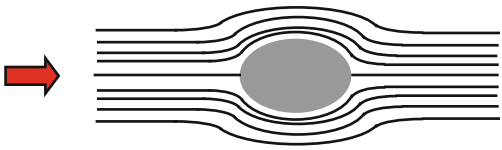

Fig. 3. Particles are subjected to fluid action

where, F is the aerodynamic drag force on the particles; CD is the drag coefficient; ρ_g is the density of the air flow; Vg and VP are gas flow velocity and particle velocity respectively; S is the upwind area of particles.

When the injection speed of powder is 0, the particles can obtain a large acceleration. If it is necessary to obtain a large acceleration, it is necessary to increase the difference between air velocity and particle velocity or reduce the powder particle size. In order to reduce the energy loss, try to avoid contact or collision between the powder and the inner wall of the nozzle. In addition, the factors affecting powder collision include powder characteristics, propulsion gas characteristics, divergent section length, spraying distance, and nozzle throat size, etc. [16]. This study mainly considers the structure. Therefore, the spraying distance, throat size, and divergent section length are selected for optimization.

Solidworks/Flow simulation module for fluid analysis is used, the influence of turbulence is considered (turbulence intensity 2%, and the inner wall conditions are adiabatic and smooth). The nitrogen (N2) is selected as the propelling gas, the internal cavity and excludes the internal non-flowing area are selected. The powder injection is selected in the low-pressure area at the junction of the throat and the divergent section.

To facilitate spraying in a small space, try to choose a shorter divergent section length. Although the shorter divergent section length is unfavorable to powder acceleration, optimizing the spraying distance can make up for the defect of insufficient divergent section length. Therefore, 4 mm, 8 mm, 12 mm, and 16 mm are selected in this paper. The spraying distance is 50 mm, nitrogen is selected as propulsion gas, and other specific fluid parameters are shown in Table 1.

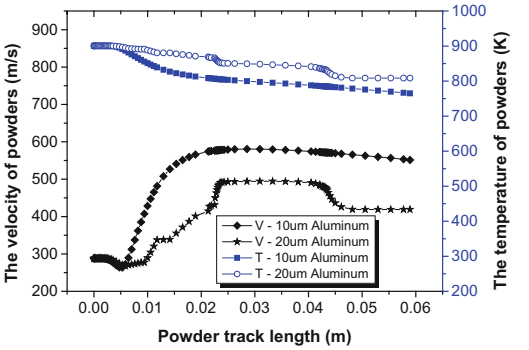

a

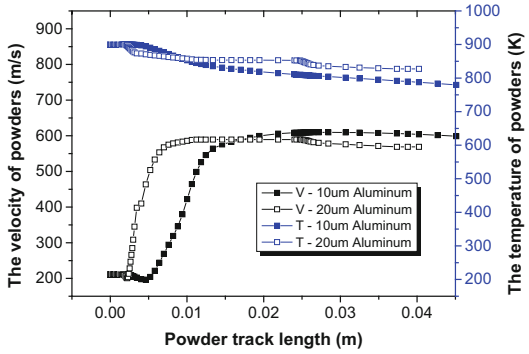

b

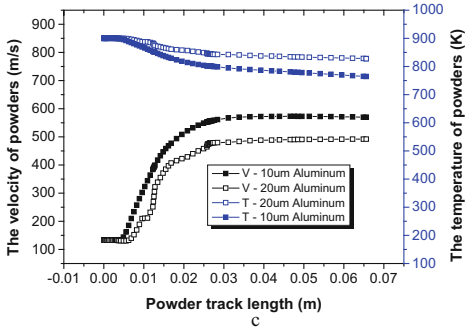

c

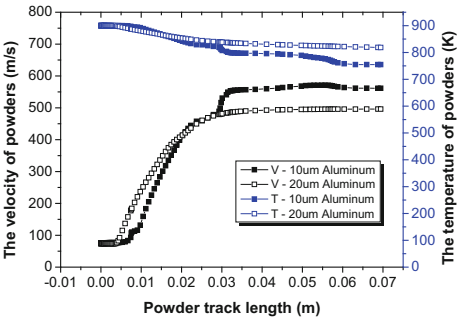

d

Fig. 4. The impact velocity and temperature changes of powder with different lengths of divergent section: a-4 mm; b-8 mm; c-12 mm, d-16 mm

Table 1. Numerical simulation parameters for different lengths of divergent segments.

Length mm	Parameters			
	Propulsion gas pressure, MPa	Propulsion gas temperature, K	Powder injection pressure, MPa	Maximum collision velocity of powder, m/s
4	5	900	0.8	1039
8	5	900	0.8	1065
12	5	900	1.2	955
16	5	900	1	1015

If the spraying distance is too large, the powder speed and powder temperature will be reduced. Figure 4 shows that the spraying distance is between 10 mm and 20 mm, and the powder has reached the maximum. The spraying distance is 10 mm (injection pressure 0.8 MPa), 15 mm (injection pressure 0.9 MPa) and 20 mm (injection pressure 0.95 MPa), the propulsion gas temperature is 900 K and the powder is 10 μm aluminum. In addition, the throat size is the key factor affecting the fluid, thus affecting the particle acceleration. According to Fig. 5, the spraying distance 15 mm is selected. Since the width of the propulsion gas inlet is 16 mm, in order to achieve the throat compression effect, the fillet is 18 mm, 22 mm and 26 mm (Fig. 6), and the powder injection pressure is 0.9 MPa.

Hence, the powder collision velocity increases with the increase of the length of the divergent section, while the powder velocity reaches the maximum when the spraying distance is basically within 20 mm, while the collision temperature decreases with the increase of particle trajectory, and the smaller the particle size, the more it decreases. However, 10 μm aluminum powder can obtain greater collision velocity than 20 μm aluminum powder under the same conditions, mainly because the obtained acceleration is greater. According to Formula (1), it is further deduced that the powder acceleration a = F/m, and the smaller the particle size, the greater the acceleration, which also explains the greater collision velocity of 10 μm powder. Figure 5 shows that the powder speed reaches the maximum when the spraying distance is 15 mm, indicating that the spraying distance should not be too short or too long. Too short will lead to the powder can not accelerate effectively, and too long will lead to the loss of powder speed. Figure 6 shows that the throat is also a key factor affecting the powder collision speed. When the fillet 18 mm increases to 22 mm, the maximum powder speed increases by about 23 m/s, while when it increases from 22 mm to 26 mm, the growth rate is less, and the maximum powder speed only increases by about 8 m/s. therefore, with the increasing fillet radius (i.e. the decreasing throat size), the growth rate of the maximum powder speed will be less and less.

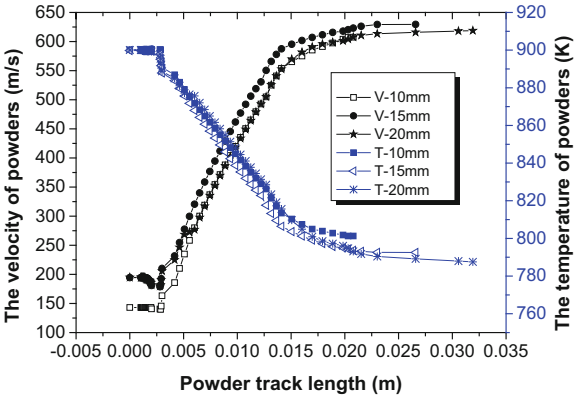

Fig. 5. Impact velocity and temperature variation of aluminum powder at different spraying distances

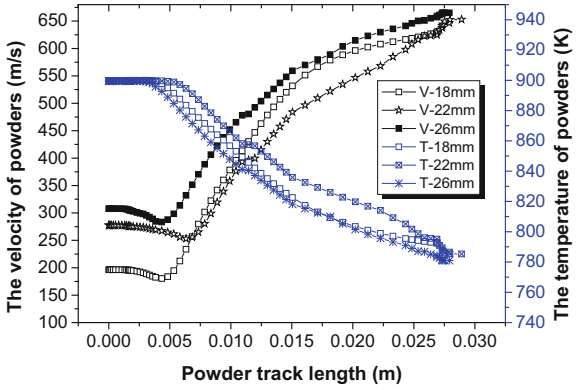

Fig. 6. Impact velocity and temperature variation of aluminum powder with different throat sizes

4 Multivariate Results and Discussion

The single factor method is commonly used by most researchers to seek rules [17], but the actual operation process is often multi-factor interaction. Therefore, multi-factor interaction analysis is more scientific and realistic.

RSM is a product of a combination of mathematics and statistical methods. It is often used to find the optimal process parameters in a multi-parameter system [18]. This study uses the Box Behnken principle to design, and the comprehensive numerical results of the single factors, three independent variables (Diffusion L, Spraying D and Fillet radius of throat R) are set through the Design-Expert software, and the powder speed is the dependent variable. A three-factor, three-level response surface quadratic regression equation is constructed. The model is Eq. 2:

$$y = \beta_0 + \sum_{i=1}^{m} \beta_i x_i + \sum_{i=1}^{m} \beta_{ij} x_j + \sum_{i=1}^{m} \beta_{ii} x_i^2 + \varepsilon \tag{2}$$

where y is the response value of the regression equation, Xi and Xj are independent variables; m is the number of independent variables, β_0 is the regression intercept; β_i is the linear effect of Xi; β_{ij} is the interaction effect of Xi and Xj; β_{ii} is the secondary effect of Xi; ε is a random error.

Input the high (+1), medium (0), and low (−1) codes and actual parameters of the independent variable into the Expert Design software, which can reduce unnecessary testing and obtain the optimal test scheme. The test methods and results are shown in Table 2.

Table 2. Test scheme and results.

Run	High and low level code			Actual value			Impact V (m/s)
	Diffusion L (mm)	Spraying D (mm)	Fillet radius of throat (mm)	Diffusion L (mm)	Spraying D (mm)	Fillet radius of throat (mm)	
1	0	0	0	8	15	22	666
2	−1	+1	0	4	20	22	578
3	0	0	0	8	15	22	666
4	+1	+1	−1	12	15	18	677
5	+1	+1	0	12	20	22	664
6	0	0	−1	8	20	18	599
7	0	0	0	8	15	22	666
8	+1	+1	+1	12	15	26	684
9	+1	+1	0	12	10	22	700
10	0	0	+1	8	20	26	630
11	0	0	0	8	15	22	666
12	−1	−1	+1	4	15	26	645
13	0	0	+1	8	10	26	675
14	−1	−1	−1	4	15	18	637
15	0	0	−1	8	10	18	643
16	−1	−1	0	4	10	22	604
17	0	0	0	8	15	22	666

As shown in Table 3, the model F-value of 7.04 and P-value of 0.0087 (less than 5%) imply the model is significant. The P-values of A and B are both less than 0.01 (less than 0.05), indicating that a single factor has a significant influence on the powder velocity, however, the P-values of C is greater than 0.05, indicating that a single factor has not a significant influence on the powder velocity. The P-value of AB, AC, and BC are both greater than 0.05, hence, the interaction between diffusion length and spraying distance, diffusion length and Fillet radius of throat, and spraying distance and fillet radius of

Table 3. Analysis of variance.

Source	Sum of squares	df	Mean square	F value	P-value
Model	15505.76	9	1722.86	7.04	0.0087
A-Diffusion L	8580.5	1	8580.5	35.08	0.0006
B-Spraying D	2964.5	1	2964.5	12.12	0.0102
C-Fillet radius of throat R	760.5	1	760.5	3.11	0.1212
AB	12.25	1	12.25	0.05	0.8293
AC	0.25	1	0.25	1.022e−3	0.9754
BC	0.25	1	0.25	1.022e−3	0.9754
A2	34.8	1	34.8	0.14	0.7172
B2	3041.12	1	3041.12	12.43	0.0096
C2	23.75	1	23.75	0.097	0.7644
Residual	1712	7	244.57		
Lack of fit	1712	3	570.67		
Error	0	4	0		
Total	17217.76	16			

throat are not obvious. The regression equation at this time is: $Y = 666 + 32.75A - 19.25B + 9.75C - 1.75AB - 0.25AC - 0.25BC - 2.88A2 - 26.88B2 - 2.37C2$. The lack of fit error is not significant. The determination coefficient of the regression equation is $R2 = 0.9006$ and the correction coefficient $R2 = 0.754$. These results indicate that the regression model can explain 90.06% of the change in powder velocity response.

It can be seen from Fig. 7 that the order of the influence of the three factors is that diffusion length is greater than spraying distance, and spraying distance is greater than fillet radius of the throat, and the maximum powder velocity is taken as the target, the optimal velocity is predicted to be 707.2 m/s (Fig. 8).

To verify the optimized parameters, import the optimized parameters into the Solidworks flow simulation module. The simulation results (Fig. 9) show that the powder velocity is 705 m/s, with an error of 0.3%. Therefore, the response surface analysis is highly accurate.

The application range of the optimized new nozzle structure is further discussed. Taking the critical velocity of powder as the standard, the critical velocity can be calculated theoretically by Eq. 3. The 10-micron size powder particles are selected, the powder is injected at room temperature, and the temperature of propulsion gas ranges from 400 k to 1200 k. Through the summary of theoretical critical velocity and numerical simulation velocity data (Table 4), the new cold spraying nozzle of this study can spray Ni, Ti, Cu, Al, Zn and Mg, which has a wide application prospect.

$$V_{\text{crit}} = \sqrt{C_P(0.7T_{\text{m}} - T_{\text{i}})} \tag{3}$$

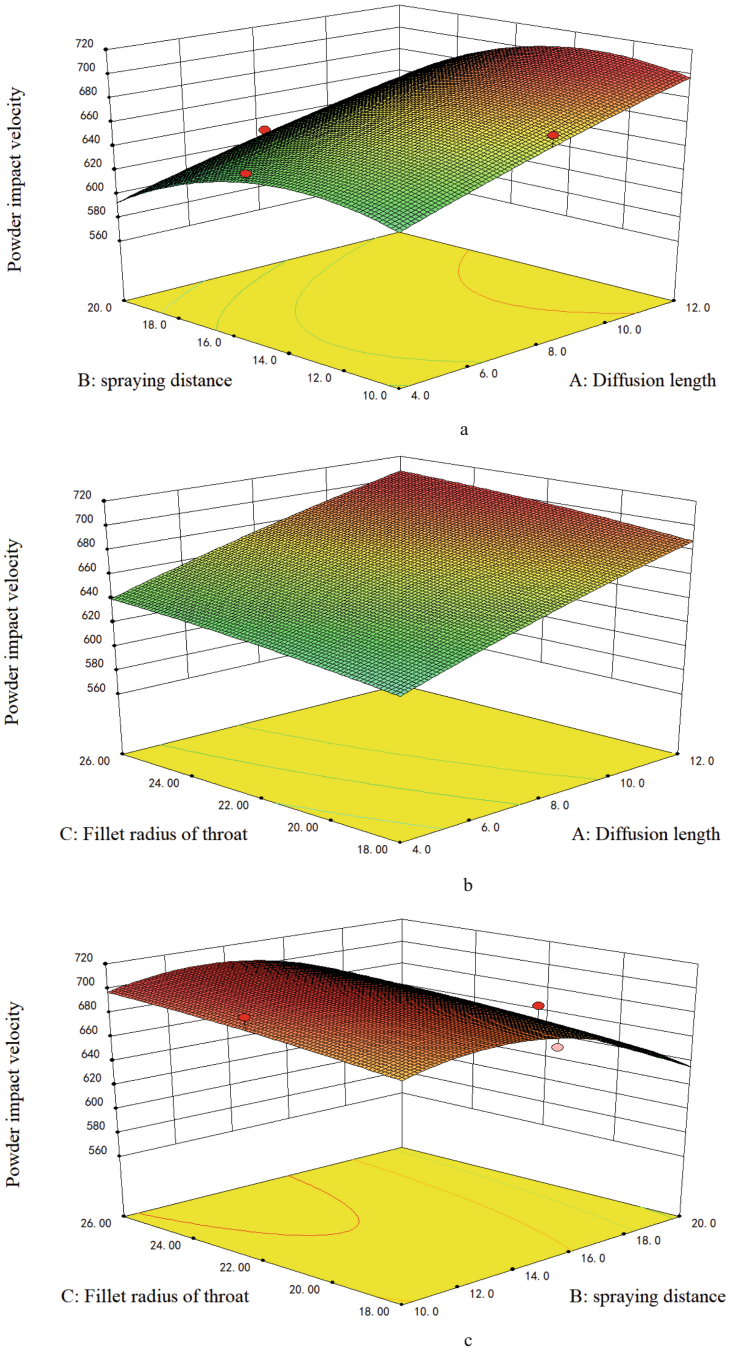

Fig. 7. Interaction effect of three factors on response under N2 conditions: a - A and B factors interaction influence; b - A and C factors interaction influence; c - B and C factors interaction influence

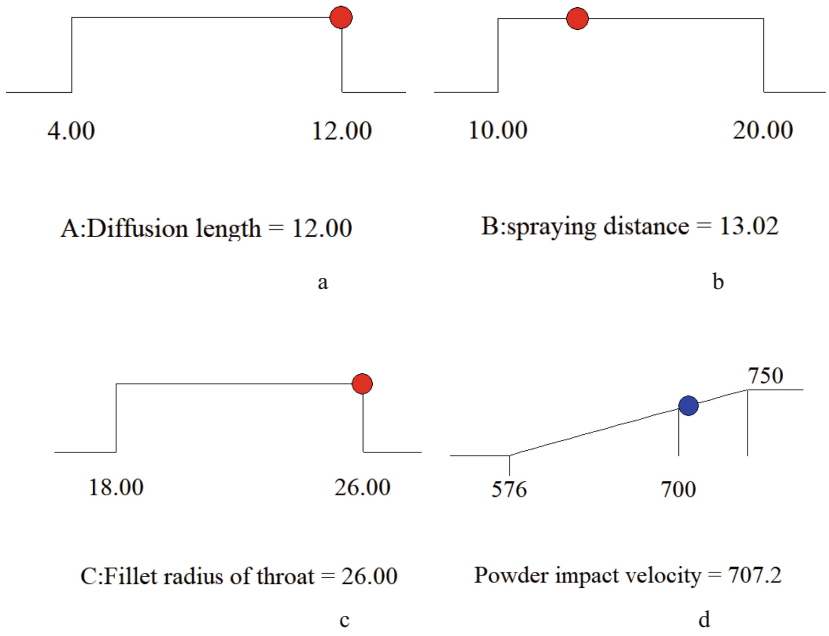

Fig. 8. Numerical simulation collision velocity under optimal parameter conditions under N2: a-optimum diffusion length; b-optimum spraying distance; c-optimum fillet radius of throat; d-response speed

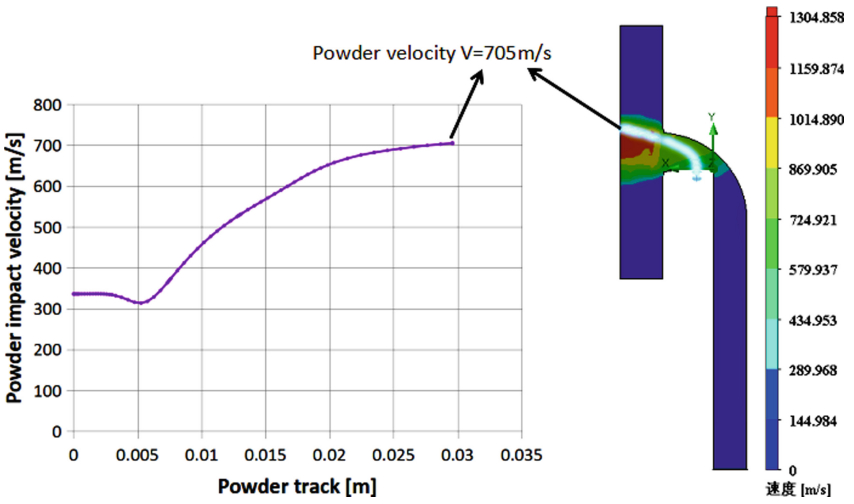

Fig. 9. Powder velocity trajectory and velocity nephogram after structure optimization

Table 4. The optimized spraying is applicable to different powder materials.

Powder parameters		Gas temperature, K								
		400	500	600	700	800	900	1000	1100	1200
Ni	Maximum speed, m/s	–	–	–	–	–	533	550	570	585
	Critical speed, m/s	–	–	–	–	–	587	574	564	552
	Whether deposition? (yes or no)	–	–	–	–	–	No	No	Yes	Yes
Ti	Maximum speed, m/s	–	–	–	587	615	640	658	680	698
	Critical speed, m/s	–	–	–	632	619	605	590	576	560
	Whether deposition? (yes or no)	–	–	–	No	No	Yes	Yes	Yes	Yes
Cu	Maximum speed, m/s	–	–	464	488	512	532	–	–	–
	Critical speed, m/s	–	–	480	467	452	437	–	–	–
	Whether deposition? (yes or no)	–	–	No	Yes	Yes	Yes	–	–	–
Al	Maximum speed, m/s	525	568	608	–	–	–	–	–	–
	Critical speed, m/s	570	544	517	–	–	–	–	–	–
	Whether deposition? (yes or no)	No	Yes	Yes	–	–	–	–	–	–
Mg	Maximum speed, m/s	562	608	652	–	–	–	–	–	–
	Critical speed, m/s	630	600	570	–	–	–	–	–	–
	Whether deposition? (yes or no)	No	Yes	Yes	–	–	–	–	–	–
Zn	Maximum speed, m/s	432	463	–	–	–	–	–	–	–
	Critical speed, m/s	299	274	–	–	–	–	–	–	–
	Whether deposition? (yes or no)	Yes	Yes	–	–	–	–	–	–	–

5 Conclusion

The RSM has certain guiding significance for multi-factor parameter optimization. The response surface model obtained by this study is reliable with an error of 0.3% and high accuracy. By analyzing the structure of cold spraying 90° rectangular nozzle, some meaningful conclusions are draws:

1. When the length of the inlet cross-sectional area of the propulsion gas is 16 mm and the width is 3 mm, that is, the cross-sectional area of the inlet is 48 mm^2, the optimal structural parameters are as follows: the length of the divergent section is 12 mm, the spraying distance is 13 mm, and the fillet radius is 26 mm. At this time, the maximum speed of 10 μm aluminum powder can reach 705 m/s.
2. The optimized 90° rectangular nozzle can meet the spraying of a variety of common metal powders with a size of 10 μm between 400 k–1200 k, which has a certain process reference value.

Acknowledgment. The authors would like to thank the China Scholarship Council for its support (NO. 202008100011).

References

1. Li, W.Y., Cao, C.-C., Yin, S.: Solid-state cold spraying of Ti and its alloys: a literature review. Prog. Mater. Sci. **110**, 1–53 (2019). https://doi.org/10.1016/j.pmatsci.2019.100633
2. Assadi, H., Gartner, F., Stoltenhoff, T., Kreye, H.: Bonding mechanism in cold gas sparing. Acta Mater. **51**, 4379–4394 (2003)
3. Hu, W.J., Markovych, S., Tan, K., Shorinov, O., Cao, T.T.: Surface repair of aircraft titanium alloy parts by cold spraying technology. Aerosp. Tech. Technol. **163**, 30–42 (2020)
4. Sun, W., Tan, A.-W.-Y., Marinescu, L., Toh, W.Q., Liu, E.: Adhesion, tribological and corrosion properties of cold-sprayed CoCrMo and Ti6Al4V coatings on 6061-T651 Al alloy. Surf. Coat. Technol. **326, part A**, 291–298 (2017). https://doi.org/10.1016/j.surfcoat.2017.07.062
5. Han, X.J.: Research on preparation of Zn-Al alloy coating on the surface of TC4 Alloy and its resistance to titanium/aluminum contact corrosion. Nanjing University of Aeronautics and Astronautics (2016)
6. Vargas-Uscategui, A., King, P.C., Styles, M.J., Saleh, M., Luzin, V., Thorogood, K.: Residual stresses in cold spray additively manufactured hollow titanium cylinders. J. Therm. Spray Technol. **29**(6), 1508–1524 (2020). https://doi.org/10.1007/s11666-020-01028-3
7. Garmeh, S., Jadidi, M., Dolatabadi, A.: Three-dimensional modeling of cold spray for additive manufacturing. J. Therm. Spray Technol. **29**, 38–50 (2020)
8. Li, W.Y., Yang, K., Yin, S., Yang, X.W., Xu, Y.X., Lupoi, R.: Solid-state additive manufacturing and repairing by cold spraying: a review. J. Mater. Sci. Technol. **34**(3), 440–457 (2017). https://doi.org/10.1016/j.jmst.2017.09.015
9. MacDonald, D., Fernandez, R., Delloro, F., Jodoin, B.: Cold spraying of Armstrong process titanium powder for additive manufacturing. Therm. Spray Technol. **26**, 598–609 (2017)
10. Wu, Z.L.: Numerical simulation research of the internal flow field cold of the spray gun nozzle and structural optimization. Henan Polytechnic University (2011)

11. Li, W.Y., Li, C.J.: Optimal design of a novel cold spray gun nozzle at a limit space. J. Therm. Spray Technol. **14**, 391–396 (2005)
12. Canales, H., Litvinov, A., Markovych, S., Dolmatov, A.: Calculation of the critical velocity of low pressure cold sprayed materials. Aircr. Des. Manuf. Issues **3**, 86–91 (2014). http://nbuv.gov.ua/UJRN/Pptvk_2014_3_11
13. Hu, W.J., Tan, K., Markovych, S., Cao, T.T., Liu, X.L.: Optimization of cold spraying 90° rectangular nozzle technological parameter via response surface analysis. Metallofizika i Noveishie Tekhnologii (2021)
14. Zho, X.L., Zhang, J.S., Wu, X.K.: Advanced Cold Spray Technology and Application. China Machinery Industry Press, Beijing (2011)
15. Hu, W.J., Tan, K., Markovych, S., Liu, X.L.: Study of cold spray nozzle throat on acceleration characteristics via CFD. J. Eng. Sci. **8**(1), 8–12 (2021)
16. Alhulaifi, A.S., Buck, G.A.: A simplified approach for the determination of critical velocity for cold spray processes. J. Therm. Spray Technol. **23**(8), 1259–1269 (2014). https://doi.org/10.1007/s11666-014-0128-8
17. Yin, S., Meyer, M., Li, W., Liao, H., Lupoi, R.: Gas flow, particle acceleration, and heat transfer in cold spray: a review. J. Therm. Spray Technol. **25**(5), 874–896 (2016). https://doi.org/10.1007/s11666-016-0406-8
18. Zhou, X.H., Wang, Y., Song, D.P., Bai, G., Li, A., Dong, Q.: Analysis and prediction on thermal conductivity of coal based on Box Behnken design. J. Saf. Sci. Technol. **13**(9), 109–115 (2017)